

Hot Plasma Environment at Jupiter: Voyager 2 Results

Abstract. *Measurements of the hot (electron and ion energies ≥ 20 and ≥ 28 kiloelectron volts, respectively) plasma environment at Jupiter by the low-energy charged particle (LECP) instrument on Voyager 2 have revealed several new and unusual aspects of the Jovian magnetosphere. The magnetosphere is populated from its outer edge into a distance of at least ~ 30 Jupiter radii (R_J) by a hot (3×10^8 to 5×10^8 K) multicomponent plasma consisting primarily of hydrogen, oxygen, and sulfur ions. Outside $\sim 30 R_J$ the hot plasma exhibits ion densities from $\sim 10^{-1}$ to $\sim 10^{-6}$ per cubic centimeter and energy densities from $\sim 10^{-8}$ to 10^{-13} erg per cubic centimeter, suggesting a high β plasma throughout the region. The plasma is flowing in the corotation direction to the edge of the magnetosphere on the dayside, where it is confined by solar wind pressure, and to a distance of ~ 140 to $160 R_J$ on the nightside at ~ 0300 local time. Beyond $\sim 150 R_J$ the hot plasma flow changes into a "magnetospheric wind" blowing away from Jupiter at an angle of $\sim 20^\circ$ west of the sun-Jupiter line, characterized by a temperature of $\sim 3 \times 10^8$ K (26 kiloelectron volts), velocities ranging from ~ 300 to > 1000 kilometers per second, and composition similar to that observed in the inner magnetosphere. The radial profiles of the ratios of oxygen to helium and sulfur to helium (≤ 1 million electron volts per nucleon) monotonically increase toward periapsis, while the carbon to helium ratio stays relatively constant; a significant amount of sodium ($\text{Na/O} \sim 0.05$) has also been identified. The hydrogen to helium ratio ranges from ~ 20 just outside the magnetosphere to values up to ~ 300 inside; the modulation of this ratio suggests a discontinuity in the particle population at ~ 50 to $60 R_J$. Large fluctuations in energetic particle intensities were observed on the inbound trajectory as the spacecraft approached Ganymede, some of which suggest the presence of a "wake." Five- and 10-hour periodicities were observed in the magnetosphere. Calculations of plasma flow velocities with the use of Compton-Getting formalism imply that plasma is mostly corotating to large radial distances from the planet. Thus the Jovian magnetosphere is confined by a plasma boundary (as was implied by the model of Brice and Ioannidis) rather than a conventional magnetopause. Inside the plasma boundary there exists a discontinuity at ~ 50 to $60 R_J$; we have named the region inside this discontinuity the "inner plasmasphere."*

We report here preliminary results from measurements made with the low-energy charged particle (LECP) instrument on Voyager 2 as it approached and traversed the magnetosphere of Jupiter. The primary objectives of the LECP instrument (1) are to make measurements of the hot plasma (≥ 20 keV and ≥ 28 keV for electrons and ions, respectively), to characterize the composition of the hot plasma and energetic particle population, and to determine the particle flows and spatial distributions. In addition, we discuss the effects associated with the possible wake of Ganymede.

The LECP instrument consists of two basic sensors. The low-energy particle telescope (LEPT) is primarily a composition instrument capable of identifying the major ion species; the low-energy magnetosphere particle analyzer (LEMPA) performs basic hot plasma (ion-electron) measurements at low and medium energies with good electron-ion separation over a large (~ 1 to 10^{11} cm $^{-2}$ sec $^{-1}$ sr $^{-1}$) dynamic range. To obtain a measure of particle anisotropies on a non-spinning spacecraft, both the sensors are mounted on a stepping motor that rotates in eight steps through 360° in time inter-

vals of 48, 192, or 384 seconds. The LECP instrument was described in (2).

Inbound pass. The LECP instrument first observed evidence of Jupiter's magnetosphere when sunward-moving ions ($E \geq 28$ keV) were observed at ~ 800 Jupiter radii (R_J) in front of the planet. This distance, more than one-third of an astronomical unit (AU), is substantially farther sunward than the first ion fluxes detected by LECP on Voyager 1 ($\sim 600 R_J$ sunward). As on Voyager 1, the frequency of occurrence of the appearance of such ions increased as Voyager 2 approached the planet.

Figure 1a shows selected electron and ion channel count rates for the inbound traversal of the magnetosphere, which began on day 184 with the first encounter of the planet's bow shock at $\sim 98 R_J$; these bow shocks are identified primarily by the change in particle flow direction. Subsequent bow shock crossings are noted, as are the Jovian plasma boundary (rather than magnetopause) crossings, which we will explain later. Also shown are the α particle to proton (p) flux ratios and the exponent γ of the electron and ion energy spectrum expressed as a power law in energy ($E^{-\gamma}$). A very brief excursion into the magnetosphere

occurred at $\sim 71 R_J$; final entry into the magnetosphere occurred at a distance of $\sim 63 R_J$ on day 186 (identified from the low-energy electron fluxes).

The p/α ratio exhibits variations over a factor of 40 with the first two maxima coinciding with the two plasma boundary crossings. However, subsequent peaks in the ratio generally correspond to relative minima in particle intensities, that is, there appear to be more protons relative to helium off the equator. Generally the p/α ratio is much larger inside the magnetosphere than either the solar wind value (~ 20 to 50) or the Jovian atmosphere value of ~ 9 (3). The electron spectra became softer while the ion spectra became harder during the two plasma boundary crossings.

Prior to closest approach, the LECP experiment was commanded into a fixed, nonstep mode wherein the low-energy ends of the LEMPA and LEPT telescopes were oriented to be almost entirely covered by the sunshade. This reduced the geometrical factors of these telescopes by up to ~ 95 percent and provided the opportunity to continue composition measurements by LEPT through spacecraft periapsis. Selected ion and electron data obtained through periapsis are plotted in Fig. 1b. Unlike the Voyager 1 inbound observations, evidence of an approximate 5-hour periodicity began to appear in the particle fluxes beginning at $\sim 33 R_J$; the periodicities persisted until $\sim 16 R_J$. Jovian particle flux periodicities were previously observed by instruments on the inbound Pioneer 10 spacecraft (4, 5). After the last dayside plasma boundary crossing (Fig. 1a) and prior to the onset of the periodicities, the fluxes, although variable, did not increase significantly with decreasing distance to the planet. At about the time of onset of the 5-hour periodicities, however, the fluxes began to increase toward their peak values reached near periapsis (Fig. 1b).

Ganymede encounter. Large fluctuations, some periodic, in the electron and ion intensities began at ~ 0400 on day 190 and terminated at ~ 1200 (all times are in SCET, spacecraft event time). The closest approach to Ganymede occurred at ~ 0714 SCET. Passage through the nominal (O_4 model) particle drift shell corresponding to the Ganymede orbit began at ~ 0741 and terminated at ~ 0821 . The spacecraft trajectory was expected to cross the Ganymede wake region ~ 1 hour after closest approach. In Fig. 2b are shown 24-second average counting rates of several electron, proton, and ion channels at a pitch angle of $\sim 90^\circ$ during

the 3-hour interval spanning the encounter with Ganymede. Also shown is the time dependence of the exponent of a power law in energy ($E^{-\gamma}$) representation of the $Z \geq 2$ spectrum. Beginning at closest approach a drop in the lowest energy electron rates was observed. Approximately 5 minutes after closest approach the electron fluxes all increased in magnitude and then began to decrease after entry into the Ganymede L-shell. Fast (~ 400 msec) time variations (not shown here) were observed in the electron fluxes near closest approach to Ganymede. The effects on the proton and ion rates are not as pronounced.

Plotted in Fig. 2a are high time-resolution rates (400 msec averages) for two electron and two ion channels for a 20-minute interval around the predicted wake passage. The data gaps in the lowest energy electron channel arise from subcommutation with another channel. The lowest energy electron rates show perturbations in the fluxes between ~ 0816 and ~ 0832 SCET. The high time-resolution rates of the other three particle channels plotted show perturbations also beginning at ~ 0816 SCET.

The LECP measurements clearly

show a direct effect of Ganymede on the Jovian electron fluxes. Ganymede is likely to be absorbing electrons. The observed structure in the intensity profiles within the postulated wake region could arise from wave-particle interactions produced by turbulence induced in the plasma by the satellite. The two peaks of electron rate variations encountered when Voyager first entered the probable wake region are similar to particle flux modulations produced by hydromagnetic waves in the earth's magnetosphere (6). In view of the intensity fluctuations before, during, and after Ganymede encounter, we do not preclude the possibility of multiple wakes.

Outbound pass. Figure 3 shows 15-minute averaged count rates of selected channels, the p/α ratio, and spectral exponents to a distance of $\sim 194 R_J$. Notable features include the double-peak structure seen on Voyager 1 and the abrupt change to a new level of minimum intensities at $\sim 57 R_J$. It is remarkable that maxima in the p/α ratio prior to $\sim 57 R_J$ coincide with intensity minima, while the reverse occurs after this distance. Similarly, the electron spectrum hardens at intensity minima (higher latitudes)

while the proton spectrum becomes softer, but beyond $\sim 57 R_J$ both spectra become harder at intensity maxima. The behavior of the p/α ratio and of the spectral parameters suggests the presence of a physically significant boundary at this distance. Similar, albeit less striking, characteristics can be found on the inbound pass (Fig. 1a) up to about the same radial distance, and in the Voyager 1 data. Thus the region inside $\sim 60 R_J$ may be a physically distinct region of the Jovian magnetosphere.

The first definitive outbound crossing of the plasma boundary (that is, change to noncorotational flow direction) occurred at $\sim 154 R_J$ with subsequent multiple crossings at $\sim 163 R_J$. After the first crossing a tailward-directed ion beam with an extremely peaked spectrum was observed. Beyond $\sim 167 R_J$, the 10-hour periodicity breaks down, and more or less continuous fluxes of particles are observed to distances $> 300 R_J$.

Composition. Figure 4 shows the abundance ratios of S, C, and O relative to He as a function of radial distance from Jupiter along both the inbound and outbound trajectories. We chose He for normalization to highlight differences be-

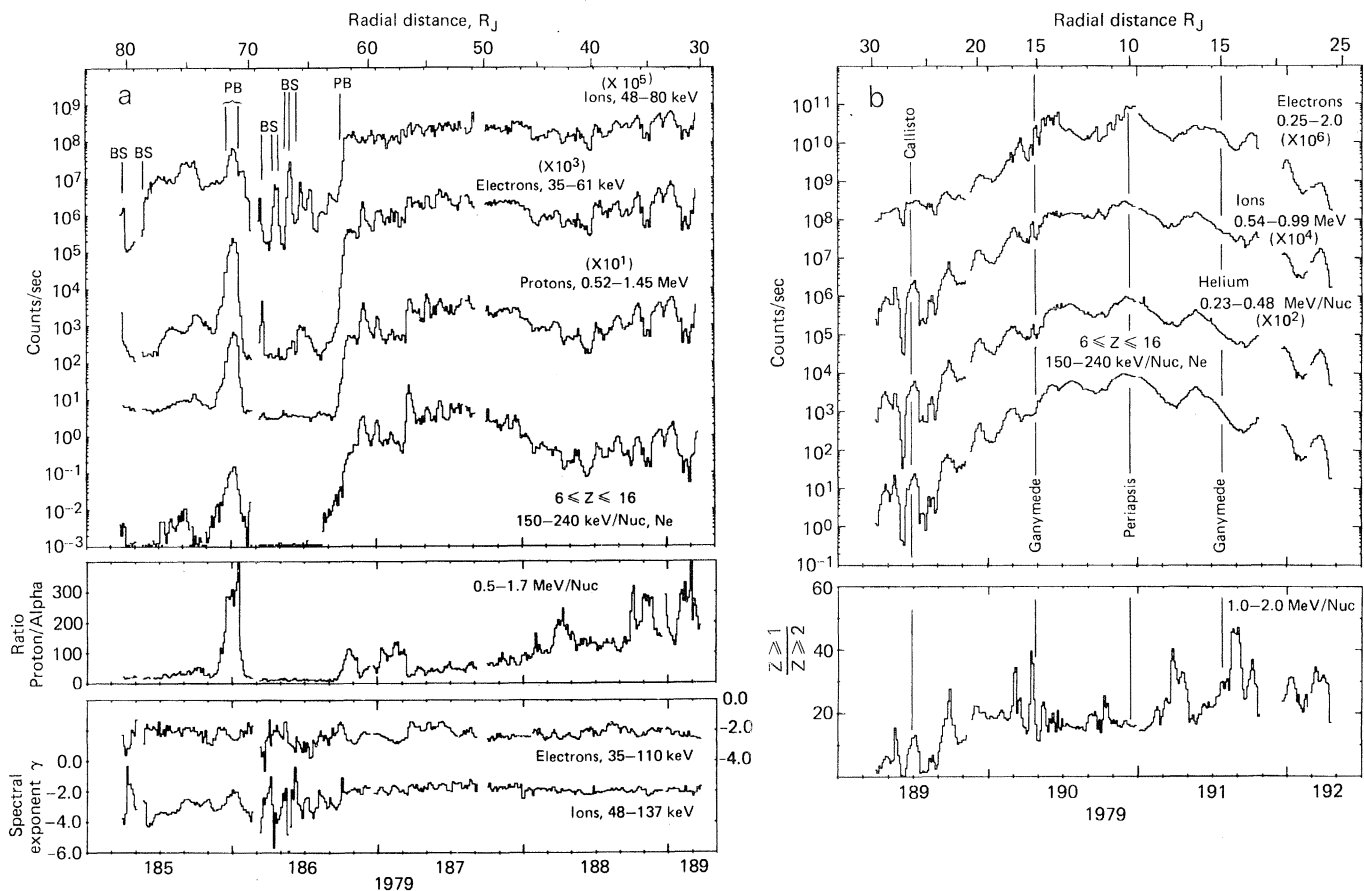


Fig. 1. (a) Inbound count-rate profiles (15-minute averages). Boundaries labeled BS (bow shock) and PB (plasma boundary) have been determined from the LECP anisotropy and rate data. Shown in the lower two panels are the proton-to-alpha ratios and the electron and ion spectral exponents. (b) Count-rate profiles (15-minute averages) inside $30 R_J$. During this interval the LECP instrument operated in a nonrotating "stow" mode. The lower panel shows count-rate ratios for the indicated ions.

tween energetic particles that probably have a source in Io's plasma torus (S and O) with those that do not (He and C).

The relative abundance of C changes little with radial distance, and the C/He ratio is similar to that in typical solar flare particle events or in the solar corona. However, both S and O show a definite increase relative to He nearer Jupiter. The O/He ratio in the outer magnetosphere is only slightly higher than solar flare or corona values while the S/He ratio is more than an order of magnitude higher than solar values, even in the outer magnetosphere.

The inset of Fig. 4 shows a typical histogram of elemental abundances in the inner magnetosphere. Within about $20 R_J$ of the planet, Na is present at about 5 percent of the abundance of O or 0.8 percent of the abundance of He. The latter value is nearly two orders of magnitude larger than solar values. The S/O ratio increases from ~ 25 percent in the outer magnetosphere to ~ 65 percent at $10 R_J$.

We conclude that in this energy range (< 1 MeV per nucleon) the C and He in Jupiter's magnetosphere have their origin in either the solar wind or the Jovian ionosphere with acceleration within the magnetosphere. The O in the outer magnetosphere could have a solar origin. However, the O in the inner magnetosphere as well as virtually all the S and Na most probably originate at Io and its plasma torus.

The smoothly varying compositional picture found by Voyager 2 within $\sim 60 R_J$ may not be typical. For example, our instrument on Voyager 1 detected an interval near the plasma boundary at $\sim 48 R_J$ that was rich in heavy elements, with ratios of S/He ~ 1 and O/He ~ 3 (1). Similarly, during a period of enhanced fluxes on day 205, when Voyager 2 was at $\sim 175 R_J$ outbound, the composition ratios were very similar to those measured at $\sim 18 R_J$.

Jovian plasma characteristics. The function of the stepping motor of the LECP is to provide information on the direction of arrival of hot plasma in the Jovian magnetosphere. The 15-minute average rates in each sector were fitted with a Fourier function, and the amplitudes and phases (as well as uncertainties) for the first and second order harmonic terms were determined during the passage of Voyager 2 through the magnetosphere. Inspection of individual angular distributions obtained at intervals of 48 and 384 seconds shows that such a representation is an accurate description of the plasma direction.

Plotted in Fig. 5 on a diagram of the

Voyager 2 trajectory through the Jovian system are arrows representing the ion (80 to 137 keV) flow magnitudes and directions at 6-hour intervals. Also shown are three representative angular intensity distributions. Upstream events prior to bow shock crossing and magnetosheath flow of the deflected solar wind are clear-

ly evident. Everywhere inside the Jovian plasma boundary the ion flows are in the direction expected of magnetospheric corotation. At distances of ~ 155 and $163 R_J$ outbound, a large change in ion flow direction toward the antisolar direction is seen. We interpret this change as coinciding with the crossing of the Jo-

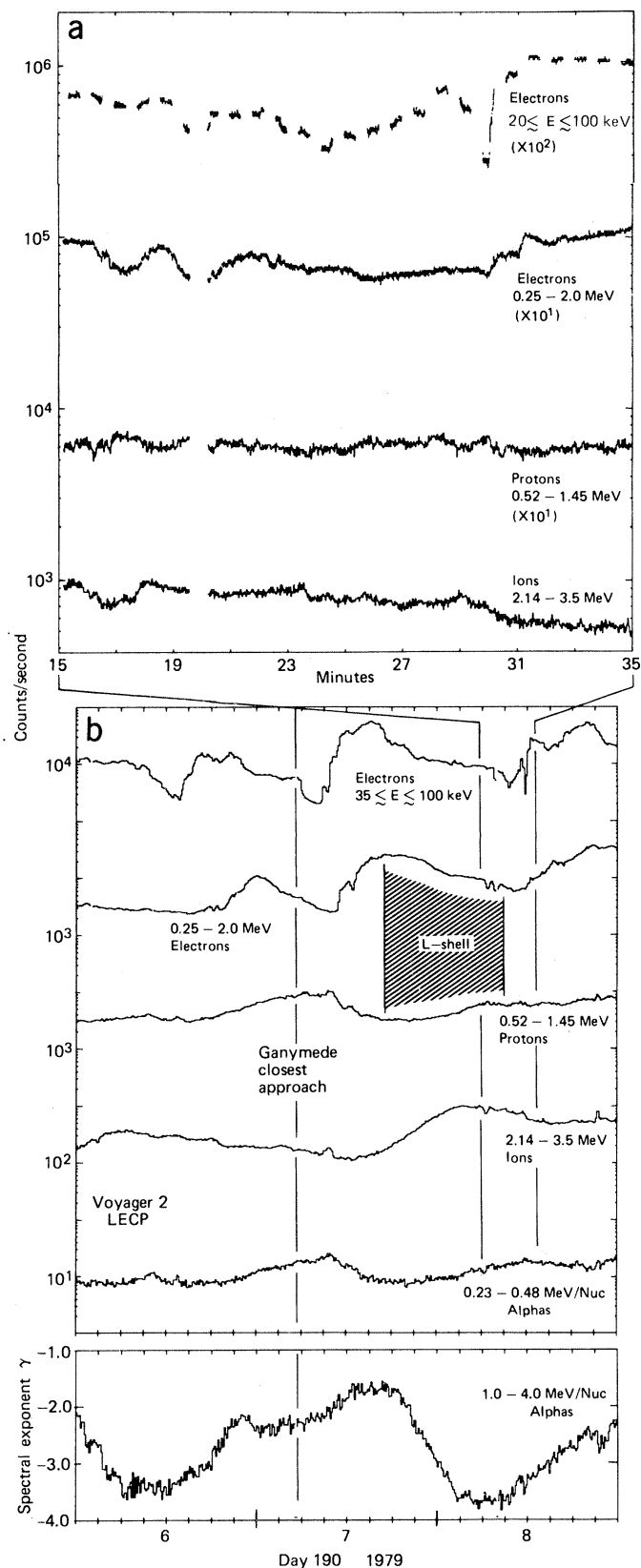


Fig. 2. Count-rate profiles for the 3 hours surrounding Ganymede's closest approach: (a) 400-msec averages during Ganymede's postulated wake passage; the two panels of (b) show 24-second averages; the L-shell region is marked according to the O_4 model. [Courtesy of Ness *et al.* (13)]

vian plasma boundary rather than a magnetopause. Similarly, on the inbound leg, we interpret the change from magnetosheath flow to one in the direction of corotation as indicative of the crossing of the dayside plasma boundary, and have so labeled it on the figure. Our Voyager 1 data (1) are consistent with these results. We note that the observed corotation is not in accord with the recent interpretation of Pioneer 10 and 11 data (7), although it agrees with earlier Pioneer results (8).

Figure 6a shows a soft spectrum obtained in the magnetosheath in sectors 6 and 4 (see inset). The large anisotropies depicted in Fig. 5 are obvious. Figure 6b shows spectra obtained at $53 R_J$ from the approximate direction of corotation (sector 6) and perpendicular to it (sector 4). A convected Maxwellian distribution with the indicated parameters has been fitted through the three lowest energy channels in sector 4, as shown. From the shape of the spectrum in both sectors it is evident that the temperature of the plasma is high. In line with our previous analysis of the Voyager 1 data (1), we can state that the majority of the ions in sector 6 are heavier ions (O and S), whereas those in sector 4 are most probably protons. A more precise estimate of the velocity (V) of the medium can be obtained by use of the linear Compton-Get-

ting transformation, which relates V to the particle anisotropy and spectrum in the spacecraft frame (measured quantities). This procedure (using ~ 600 -keV protons) yields a mean value of $\sim 620 \pm 100$ km/sec; this may be compared with the corotational velocity of 667 km/sec at this radial distance.

Figure 6c shows spectra at $32.5 R_J$, together with a Maxwellian fit in sector 4; it is obvious that the temperature, anisotropy, and velocity have decreased. The estimated velocity in this case is ~ 416 km/sec, compared to a corotational velocity of 409 km/sec. Figure 6d shows spectra at $81 R_J$ of the outbound pass, together with the changed relative positions of the sun and Jupiter in the LECP sectoring scheme. Again, the anisotropies are large with maximum fluxes from the corotation direction (sectors 4 and 3). Assuming that the flux in sector 2 is primarily protons, we obtain the indicated temperature, density, and velocity in a Maxwellian distribution. Using this fit, we can predict the proton contribution to sector 4, subtract these from the observed number, and obtain the heavy ion intensities that are shown in Fig. 6e. Inspection of the pulse-height analysis matrix at higher energies reveals that oxygen ions dominate at this time. We see from the Maxwellian fit that heavy ion densities are twice those of

protons for a total density of $\sim 10^{-3} \text{ cm}^{-3}$. The velocities are large but somewhat less than the corotational value of ~ 1020 km/sec.

Figure 6f shows a spectrum at a radial distance of $\sim 185 R_J$, when the flow direction had changed away from corotation and was pointing in the tailward direction. Again, significant anisotropies exist, and the spectra exhibit the characteristic low-energy flattening indicative of a high temperature. A Maxwellian fit to the data in sector 3 (perpendicular to the flow direction) gives the indicated values of temperature, density, and velocity. Examination of a pulse-height matrix at higher energies during this general period reveals that the composition is very similar to that shown in Fig. 4 at $\sim 18 R_J$, that is, the origin of this plasma is, by inference from the higher energies, magnetospheric. Overall, the energy spectra examined so far (many more than shown here) within the Jovian magnetosphere show a flattening or peak at low energies, and can be characterized as convected Maxwellians (with a high-energy tail) at temperatures ranging from ~ 20 to ~ 40 keV. This result is in strong disagreement with recent work (9) suggesting temperatures in the 1 to 10 keV range for the Pioneer 10 and 11 encounters.

To examine further the implications of

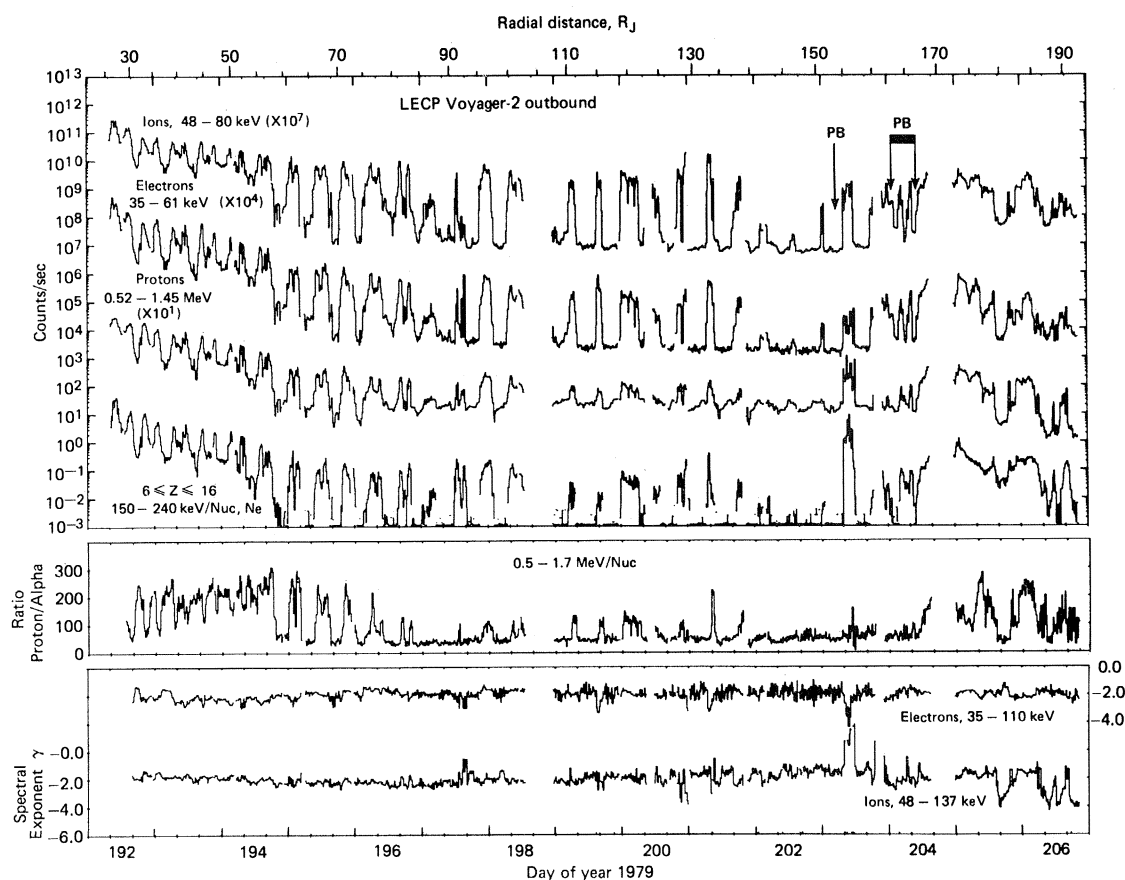


Fig. 3. Count-rate profiles (15-minute averages) for the outbound trajectory in the same format as Fig. 1a.

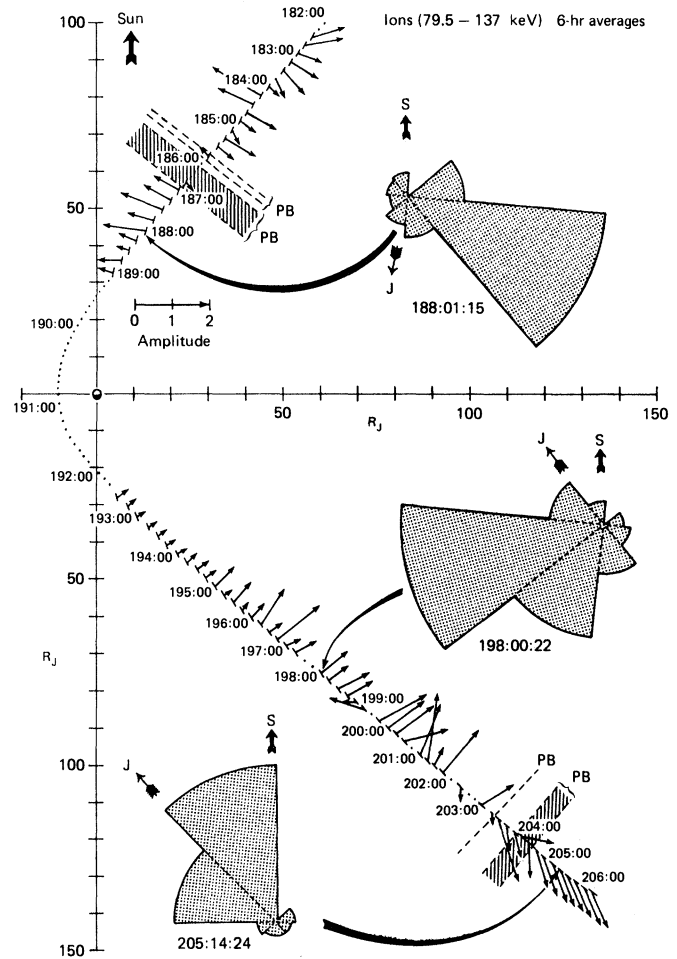
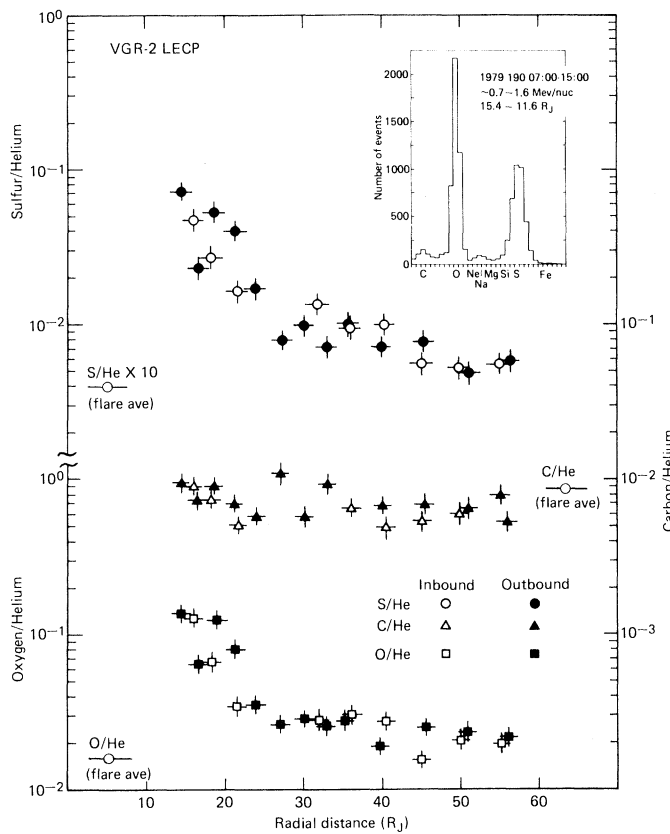


Fig. 4. Abundance ratios of S, C, and O relative to He at equal energy per nucleon as a function of distance from Jupiter. The energy intervals are 0.60 to 0.95 MeV per nucleon outside $20 R_J$ and 0.77 to 1.15 MeV per nucleon inside $20 R_J$. Average values of the three ratios in solar flare particle events (21) are indicated for comparison. The insert shows a typical composition histogram in the inner magnetosphere. Fig. 5. First-order anisotropies along the Voyager 2 trajectory. The intensity diagrams indicate typical angular distributions of observed count rates. The 45° sector clockwise from the solar direction is permanently blocked so that no measurements are possible. The small vectors after periapsis and prior to day 196 are partly due to a change in the orientation of the LECP scan plane away from the ecliptic.

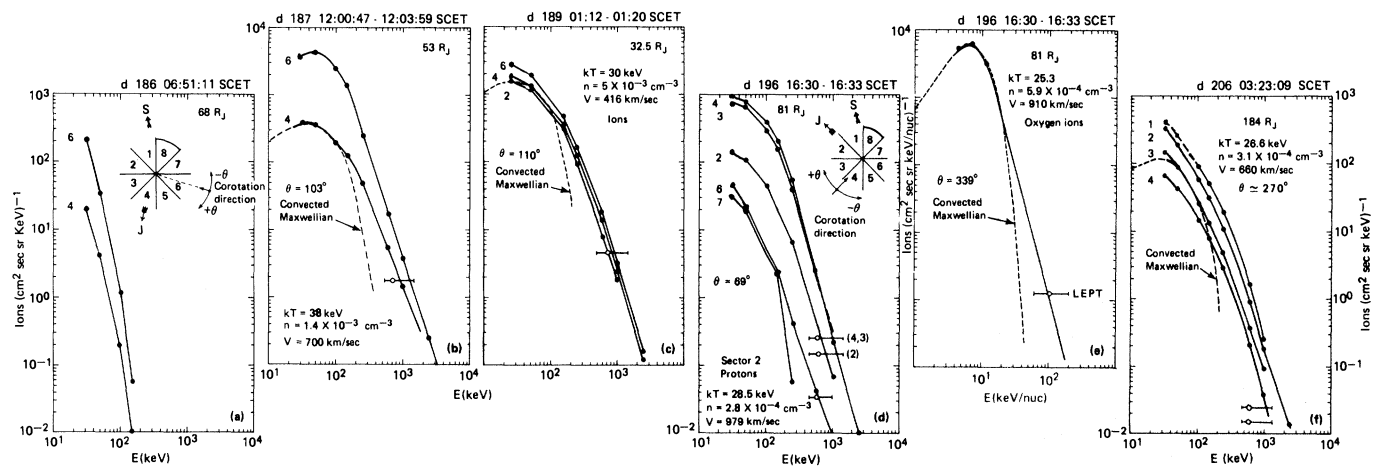


Fig. 6. Typical energy spectra obtained at various radial distances in the Jovian magnetosphere. The convected Maxwellian distributions are determined by fitting the expression

$$j(\epsilon, \theta) = C \exp \left\{ - \frac{\epsilon M}{kT} \left[1 - 2 \left(\frac{\epsilon_c}{\epsilon} \right)^{1/2} \cos \theta + \frac{\epsilon_c}{\epsilon} \right] \right\}$$

where M is particle mass number and $\epsilon_c = 1/2 V_c^2$, V_c = corotating velocity. The open circles indicate a proton (rather than $Z \geq 1$) intensity measurement for indicated sectors.

this hot, moving plasma, we have computed the number and energy densities in the range of 28 to 540 keV during the inbound and outbound passes, assuming that the scan-averaged intensity measured over ~ 3.5 sr is an accurate sample over the whole sphere (4π). To simplify the computation, we have assumed two extreme cases: (i) That all ions are protons, which gives a lower limit to the measured densities or (ii) that all ions are oxygen, which gives a probable upper limit to the measured densities in this energy range. The results are shown in Figs. 7 and 8 for the inbound and outbound passes, respectively.

The upper curve in Fig. 7 shows the density profile, with the left-hand scale appropriate for an all-proton plasma and the right-hand scale for an all-oxygen plasma; similarly, the lower curve gives the energy density. The open circles are electron densities deduced from plasma wave measurements (10). We note that the electron densities are generally higher than those for a proton plasma, but mostly lower than those of an oxygen plasma. Given our composition measurements, the probable density is in between the two, that is, in reasonable agreement with the electron density measurements. The implication of this

comparison is that most of the plasma lies above the energy threshold of the LECP at ~ 28 keV.

Considering the energy density curve, we note that after the inbound plasma boundary crossing, the energy density is comparable to that in a 7-nT magnetic field, even if the plasma is all protons. Judging from the magnetic field magnitudes seen on Voyager 1 (11), we suggest that the boundary is determined by the balance of solar wind pressure with magnetosphere plasma pressure, rather than with planetary magnetic field pressure. In this sense, the limit of the Jovian magnetosphere is not a magnetopause but rather a plasmopause, as predicted by Brice and Ioannidis (12).

Figure 8 shows similar data for the outbound pass; densities at $\sim 10^{-6} \text{ cm}^{-3}$ are instrument background. Again, we note the good comparison between the electron densities (10) and the observed ion densities, suggesting that in the nightside plasma sheet there is little plasma below the LECP threshold. The energy density of the hot plasma is again comparable to that in a 5-nT magnetic field outside $\sim 57 R_J$, and if a significant fraction of the ions is oxygen and sulfur, it is possible that the hot plasma dominates the field within the plasma sheet. The discontinuity in the energy density profile at $57 R_J$ is in the vicinity of an abrupt decrease in the magnetic field magnitude observed by Voyager 1 (11). We note the large energy densities following the boundary crossings on day 203, which at times exceed the 5-nT equivalent. In this region of space Ness *et al.* (13) give values of 2 to 4 nT, that is, the magnetic field is dominated by the plasma (frozen in) and is carried away from the planet in the form of a "magnetospheric wind."

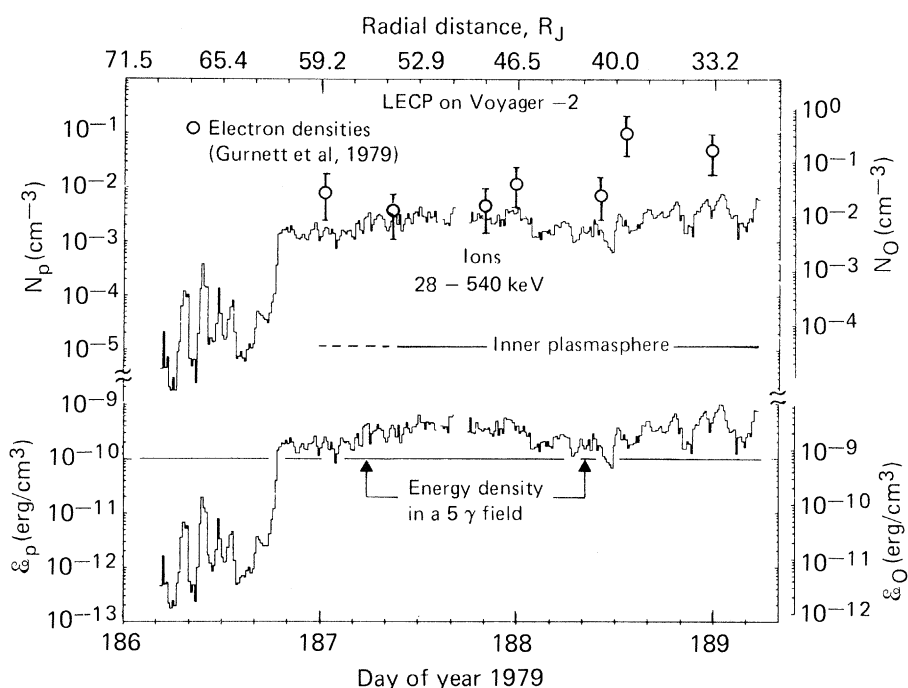


Fig. 7. Particle- and energy-density profiles (15-minute averages), derived by integration of spectra such as those shown in Fig. 5 at $E \geq 28$ keV, for the inbound pass. Open circles represent plasma wave measurements of the electron number densities (10) and refer to the left-hand scale.

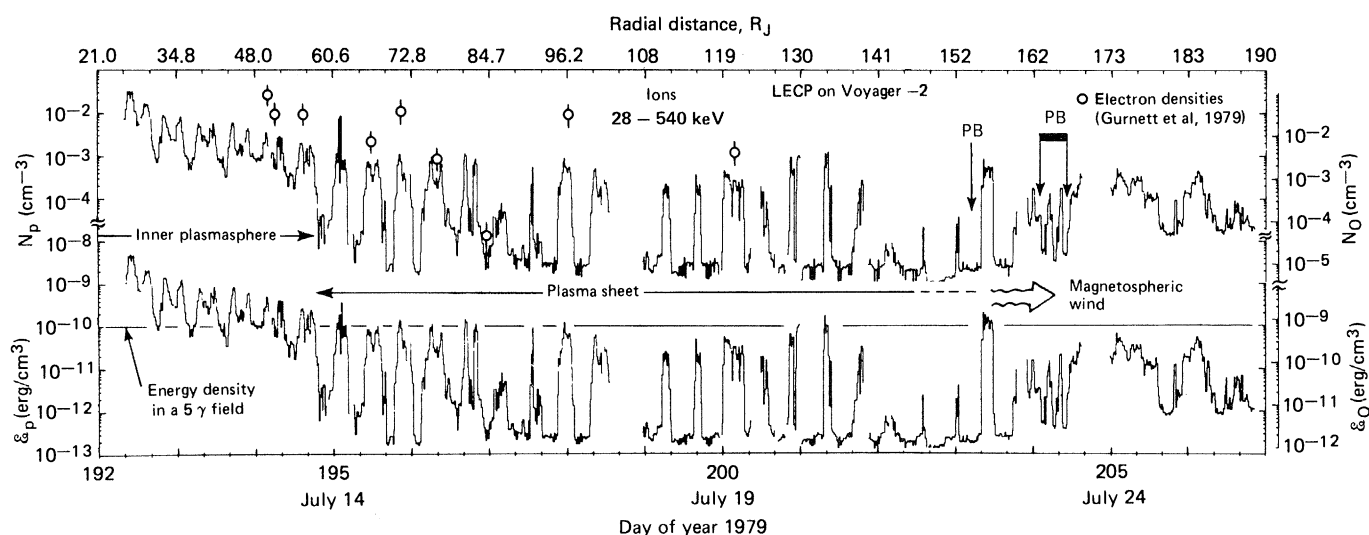


Fig. 8. Similar to Fig. 7 but for the outbound pass. Designated regions are explained in the text and refer to Fig. 9.

Discussion. The hot plasma data returned by the LECP instruments on Voyager 1 and 2 can be used to draw important conclusions about Jupiter's magnetosphere. Proposed phenomenological, qualitative models for the magnetosphere have been reviewed in (14-16). The magnetic anomaly model (14) does not appear to predict the observed particle flux periodicities, or hot plasma flow directions. Models of fast radial outflow of plasma outside the Alfvén surface, as in theories of stellar winds (15, 16), do not appear to fit the Voyager 2 data. The observed flow is generally corotational out to the plasma boundary, although a small radial component cannot be excluded.

As noted in (1) and as is emphasized by the hot plasma number and energy densities of Fig. 7, the Jovian dayside magnetospheric boundary is apparently determined by a pressure balance between the solar wind plasma and the hot Jovian plasma. The energy density in an 8-nT Jovian magnetic field at the boundary (11) is essentially equal to the energy density of an $\sim 2 \times 10^{-3} \text{ cm}^{-3}$ hot proton plasma (Fig. 7). This is a boundary situation rarely encountered at Earth's magnetopause, where the standoff distance is determined to first order by the vacuum magnetic field of Earth. This fact, coupled with the observation of plasma flowing in the corotation direction and the observed corotational velocities, dictates that the Jovian magnetosphere boundary is actually a plasma boundary. This unusual boundary condition undoubtedly causes the large spatial variations in the Jovian plasmapause; a small decrease in the solar wind pressure will cause the boundary suddenly to become unstable. A large volume of hot, previously corotating, $\beta > 1$ plasma can be lost to interplanetary space, produce the upstream ion and electron bursts, and become "thermalized" by the much denser solar wind plasma. The magnetosphere plasma would be resupplied by its internal plasma sources.

The hot plasma measurements on the outbound trajectories of both Voyagers give important clues to the structure of the nightside Jovian magnetosphere. A qualitative plasma model of the magnetosphere in the equatorial and meridional planes is shown in Fig. 9. The early plasma boundary locations of both Voyager spacecrafts are shown. The most significant features are that Voyager 2 observed the nightside plasma boundary crossings occurring at much closer distances than would be expected from all proposed models (15) and that plasma

flows are observed in the corotational direction as far as $\sim 155 R_J$. The odd-shaped plasma boundary should not be unexpected, in that the solar wind takes well over a planetary rotation period to traverse the distance from $\sim 100 R_J$ ahead of to $\sim 150 R_J$ behind Jupiter. Thus solar wind inhomogeneities may lead directly to local instabilities in the plasma boundary surface. The relation between the plasma boundary and the magnetosheath is not clear. A magnetopause may exist coincident with, or far beyond the boundary surface.

Just outside this plasma boundary, however, a most remarkable phenomenon takes place. Hot Jovian plasma breaks away from corotational flow and begins to move tailward in an essentially continuous stream, with velocities ranging from ~ 300 to over 1000 km/sec (17);

its energy density is often larger than that of the magnetic field (13), that is, the field is "frozen in." We have named this phenomenon the magnetospheric wind. The wind persists to at least $\sim 300 R_J$ in this region of the Jovian magnetosphere, but its density decreases with distance. As indicated in Fig. 9, a and b, the wind probably extends behind Jupiter as well in a region from which the magnetosheath solar wind plasma is excluded.

The interplanetary magnetic field has been ignored in the above discussions. It is not clear how the classical ideas of magnetic field-line merging, as applied to the case of the earth's magnetopause, would apply to the case of Jupiter, where the plasma β at the plasma boundary is always > 1 and where the bulk plasma is very tenuous and very hot.

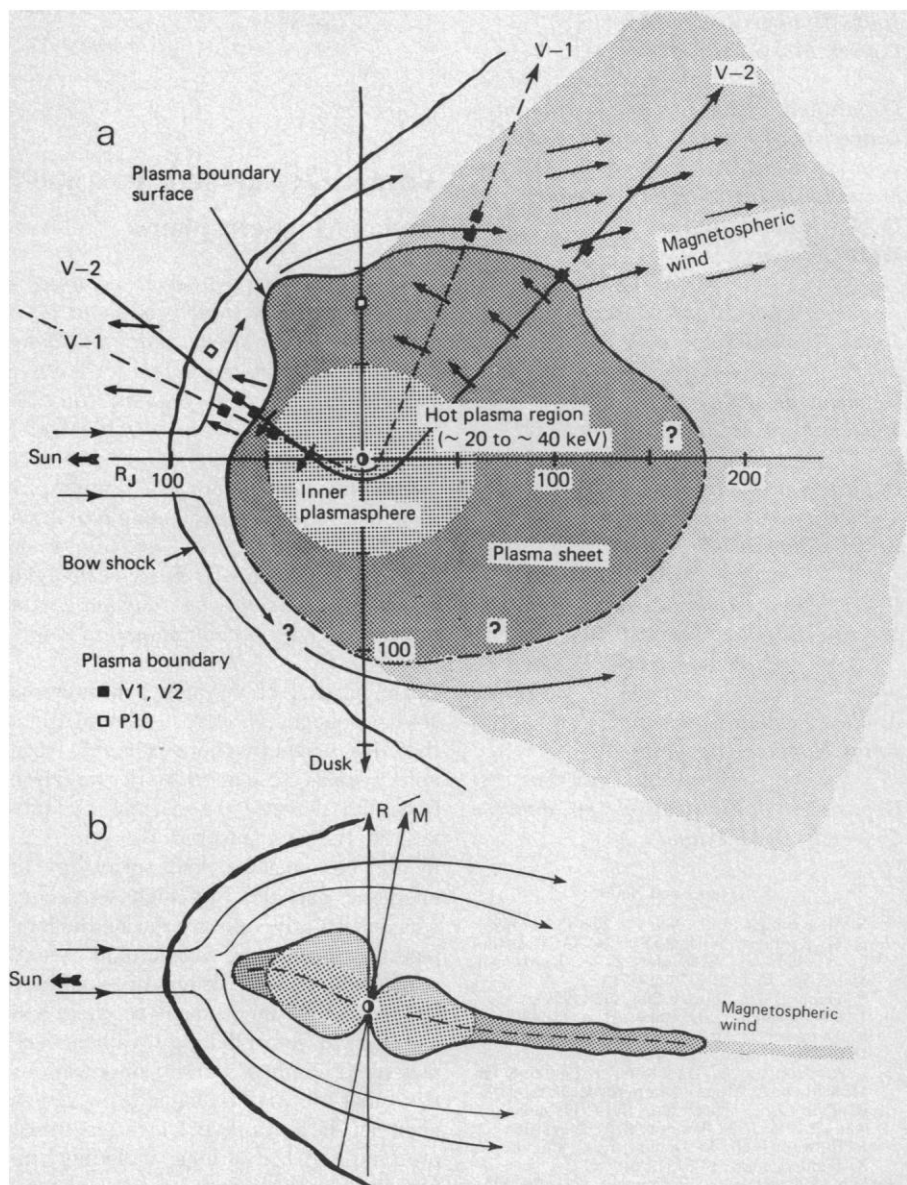


Fig. 9. Plasma model of the Jovian magnetosphere in (a) the equatorial and (b) the meridional planes. The model emphasizes the hot plasma regions. Question marks indicate areas of uncertainty. The long arrows indicate solar wind flow direction.

The model sketched in Fig. 9a for the Jovian equatorial plane magnetosphere resembles in its plasma flow patterns the Jovian magnetosphere model discussed a decade ago by Brice and Ioannidis (12); that model, however, did not include either the wind or the hot plasma. We have not discussed the mechanisms for generating a convection electric field, particularly if magnetic merging at the plasma-pause is not important, nor the effects of such a field. The shapes of possible Jovian current sheets have been discussed previously (4, 15, 18, 19). In view of our results, acceleration mechanisms proposed to date that are predominantly "single-particle" (20) are not capable of raising the bulk temperature of the magnetospheric plasma to the values we have measured.

S. M. KRIMIGIS

Applied Physics Laboratory,
Johns Hopkins University,
Laurel, Maryland 20810

T. P. ARMSTRONG

Department of Physics and Astronomy,
University of Kansas, Lawrence 66044

W. I. AXFORD

Max-Planck Institute for Aeronomy,
D-3411 Katlenburg-Lindau 3,
West Germany

C. O. BOSTROM

Applied Physics Laboratory,
Johns Hopkins University

C. Y. FAN

Department of Physics,
University of Arizona, Tucson 85721

G. GLOECKLER

Department of Physics and Astronomy,
University of Maryland,
College Park 20742

L. J. LANZEROTTI

Bell Telephone Laboratories,
Murray Hill, New Jersey 07974

E. P. KEATH, R. D. ZWICKL

J. F. CARBARY

Applied Physics Laboratory,
Johns Hopkins University,

D. C. HAMILTON

Department of Physics and Astronomy,
University of Maryland

References and Notes

1. S. M. Krimigis *et al.*, *Science* **204**, 998 (1979).
2. S. M. Krimigis, W. I. Axford, C. O. Bostrom, C. Y. Fan, G. Gloeckler, L. J. Lanzerotti, *Space Sci. Rev.* **21**, 329 (1977).
3. R. Hanel *et al.*, *Science* **204**, 972 (1979).
4. J. A. Van Allen, D. N. Baker, B. A. Randall, M. F. Thomsen, D. D. Sentman, H. R. Flindt, *ibid.* **183**, 309 (1974).
5. J. A. Simpson, D. Hamilton, G. Lentz, R. B. McKibben, A. Mogro-Campero, M. Perkins, K. R. Pyle, A. J. Tuzzolino, J. J. O'Gallagher, *ibid.*, p. 306; J. H. Trainor, B. J. Teegarden, D. E. Stilwell, F. B. McDonald, E. C. Roelof, W. R. Webber, *ibid.*, p. 311.
6. J. N. Barfield *et al.*, *J. Geophys. Res.* **76**, 5252 (1971).
7. F. B. McDonald, A. W. Scharadt, J. H. Trainor, *ibid.* **84**, 2579 (1979).
8. J. A. Van Allen, in *Jupiter*, T. Gehrels, Ed. (Univ. of Arizona Press, Tucson, 1976).

9. C. K. Goertz, A. W. Scharadt, J. A. Van Allen, J. L. Parish, *Geophys. Res. Lett.* **6**, 495 (1979).
10. D. A. Gurnett, W. S. Kurth, F. L. Scarf, *Science* **206**, 987 (1979).
11. N. F. Ness, M. H. Acuna, R. P. Lepping, L. F. Burlaga, K. W. Behannon, F. M. Neubauer, *ibid.* **204**, 982 (1979).
12. N. M. Brice and G. A. Ioannidis, *Icarus* **13**, 173 (1970).
13. N. F. Ness, M. H. Acuna, R. P. Lepping, L. F. Burlaga, K. W. Behannon, F. M. Neubauer, *Science* **206**, 966 (1979).
14. A. J. Dessler and V. M. Vasyliunas, *Geophys. Res. Lett.* **6**, 37 (1979).
15. C. F. Kennel and F. V. Coroniti, *Annu. Rev. Astron. Astrophys.* **15**, 389 (1977).
16. F. C. Michel and P. A. Sturrock, *Planet. Space Sci.* **22**, 1501 (1974).
17. We note that at the interface where magnetospheric plasma is moving in the corotation direction and solar wind plasma in the tailward direction, one should expect excitation of large plasma instabilities and possibly a boundary layer. Evidence for such effects is seen at ~ 0800 to 1200 hours on day 203, where a tailward plasma beam exhibits a sharply peaked spectrum with maximum intensity at an energy of ~ 150 keV. In addition, large dawn-to-dusk asymmetries over the entire magnetosphere should be expected.
18. E. J. Smith, L. Davis, Jr., D. E. Jones, D. S. Colburn, P. J. Coleman, Jr., P. O. Dyal, C. P. Sonnett, *Science* **183**, 305 (1974); E. J. Smith, L. Davis, D. E. Jones, P. J. Coleman, D. S. Colburn, P. Dyal, C. P. Sonnett, A. M. A. Frandsen, *J. Geophys. Res.* **79**, 350 (1974).
19. C. K. Goertz, *J. Geophys. Res.* **81**, 3368 (1976).
20. A. Nishida, *ibid.*, p. 1771; C. K. Goertz, *ibid.* **82**, 3145 (1978).
21. G. Gloeckler, *Rev. Geophys. Space Phys.* **17**, 569 (1979).
22. We thank the Voyager Project Office, JPL, and the Planetary Programs Office, NASA Headquarters, for help and cooperation in carrying out this experiment. We thank D. P. Peletier, S. A. Gary, R. G. King, J. W. Kohl, D. E. Fort, J. T. Mueller, J. H. Crawford, R. E. Thompson, B. A. Northrop, and J. Hook at JHU/APL; J. Cain, E. Tums, and R. Lundgren of the University of Maryland, C. G. MacLennan of Bell Laboratories, and J. O'Donnell, R. P. Briggs, R. B. Decker, S. T. Branden, J. H. Nonnast, F. Kutchko, and M. Paonessa of the University of Kansas for their enthusiasm and long hours that made the LECP experiment a success. The work of E. Franzgrote and D. Griffith of JPL (among many others) was essential to the success of our investigation. We thank R. E. Gold of JHU/APL for assistance and valuable suggestions; A. J. Dessler of Rice University and A. Cheng of Bell Laboratories for discussions; D. A. Gurnett and N. F. Ness for information on their data prior to publication; the referees, several colleagues, and especially F. L. Scarf for valuable suggestions. The LECP program was supported at JHU/APL by NASA under Task I of contract N00024-78-C-5384 between the Johns Hopkins University and the Department of the Navy and by subcontract at the Universities of Kansas, Maryland, and Arizona. This report presents the results of one phase of research carried out with JPL under NASA contract NAS 7-100.

19 September 1979

Voyager 2: Energetic Ions and Electrons in the Jovian Magnetosphere

Abstract. *The Voyager 2 encounter has enhanced our understanding of earlier results and provided measurements beyond 160 Jupiter radii (R_J) in the magnetotail. Significant fluxes of energetic sulfur and oxygen nuclei (4 to 15 million electron volts per nucleon) of Jovian origin were observed inside 25 R_J , and the gradient in phase space density at 12 R_J indicates that the ions are diffusing inward. A substantially longer time delay versus distance was found for proton flux maxima in the active hemisphere in the magnetotail at Jovicentric longitudes $\lambda_{III} = 260^\circ$ to 320° than in the inactive hemisphere at $\lambda_{III} = 85^\circ$ to 110° . These delays can be related to the radial motion of plasma expanding into the magnetotail, and differences in the expansion speeds between the active and inactive hemispheres can produce rarefaction regions in trapped particles. It is suggested that the 10-hour modulation of interplanetary Jovian electrons may be associated with the arrival at the dawn magnetopause of a rarefaction region each planetary rotation.*

The passage of Voyager 2 through the Jovian magnetosphere demonstrated that this magnetosphere is highly variable, even as close as 10 Jupiter radii (R_J) from the planet. The cosmic-ray subsystem (CRS) measured the flux, elemental composition, and anisotropy of energetic particles. Its high sensitivity was particularly valuable during the long passage through the magnetotail, where particle fluxes were orders of magnitude less than in the inner magnetosphere and approached interplanetary values. The new data confirm earlier observations (1-4) that the Jovian magnetosphere is a giant accelerator of particles—electrons, protons, and heavy ions, including sulfur. We observed both spatial and temporal changes in the magnetosphere as compared to prior observations with Pioneer 10 and 11 (2, 3, 5) and Voyager 1 (1).

Energetic particle morphology. After final entry into the subsolar hemisphere at 61.5 R_J (6), proton and electron fluxes observed during the inbound pass (Fig. 1) were in general consistent with earlier observations (1-3). One difference with Voyager 1 observations, both inbound and outbound, however, was the smooth change with distance of proton intensity maxima inside 35 R_J . These maxima occur at magnetic equatorial crossings which fall alternately at Jovicentric longitudes $\lambda_{III} \sim 100^\circ$ and $\sim 300^\circ$ (Fig. 1). In the case of Voyager 1, crossings in the active hemisphere ($\lambda_{III} \sim 300^\circ$) (7) were substantially more intense (1) than in the inactive hemisphere ($\lambda_{III} \sim 100^\circ$).

As shown in Fig. 2, the proton flux ($E > 2.5$ MeV) was unusually variable between 17 and 13 R_J on the inbound pass, a period which falls within ± 4